Revista Brasileira de Física, Vol. 3, N.° 2 , 1973

# The Acquisition of Raman Data of Macromolecules in Solution

JAMES E. MOORE and LEWIS M. FRAAS
Instituto de Física+ "Gleb Wataghin", Universidade Estadual de Campinas, Campinas SP

Recebido em 14 de Dezembro de 1972

It is shown that the acquisition of Raman data of macromolecules, even in the presence of a fluorescence background, can be obtained with a good signal to noise ratio and the value of such data is pointed out. Two novel approaches are also suggested that enable the experimenter, in one case, to minimize the fluorescence background through selective phonon enhancement and, in the other case, to obtain more information about macromolecular phonon modes by means of an electro-Raman-effect.

Mostramos que a obtenção de dados de efeito Raman em macromoléculas pode ser conseguida mesmo na presença de um fundo fluorescente, com uma boa razão sinal/ruido. O valor desses dados é discutido' São também sugeridos dois novos métodos que possibilitam ao experimentador, em um caso, a minimizar o fundo fluorescente por meio da intensificação seletiva de fonons; em outro caso, a obter mais informação sobre modos de fonons macromoleculares, através de um efeito Raman eletrônico.

## Introduction

Until the advent of the laser, the Raman spectroscopic technique, when. used for the elucidation of structure of molecules of biological interest, had been severely restricted for the following experimental reasons: a) small sample size, b) sample photosensitivity, c) absorption heating, and d) fluorescence interference. However, with the advent of the laser, most of the aforementioned problems have been solved. For example, Beattie[1] has reported Raman data from a 0.1 mg sample of octasulfur. Without a laser, a sample size of at least an order of magnitude greater would be required. The problems of photosensitivity and optical absorption can be minimized by the proper selection of excitation frequency. As an example, some compounds may be highly absorbtive or photosensitive to radiation at shorter wavelengths but rather unperturbed by red radiation.

The use of the laser has aided in the reduction of interference from fluorescence as well. Still, fluorescence interference is presently the greatest

+Postal address: C.P. 1170, 13100-Campinas SP

problem in the successful recording of Raman data for large molecules. The present paper is mainly concerned with experimental methods of reducing fluorescence interference.

Some successful Raman experiments have been reported where a large fluorescence background exists[2,3] and M. Tobin[4] has discussed the intrinsic signal to noise ratio for a spontaneous Raman signal superimposed on a large fluorescence background. We begin this paper in Section 1 with a summary of Tobin's method of Raman data acquisition. In Section 2, we propose a radical departure from the Tobin approach. The experimental method of Section 2 is based on the fact that no fluorescence is found on the anti-Stokes side of the exciting line. In the spontaneous Raman effect, thermal equilibium exists and Raman signals in the anti-Stokes region are negligible. If, however, phonon population can be selectively enhanced, then thermal equilibrium will no longer prevail and Raman signals will be found without fluorescence interference. In the method of Section 2, the selective phonon population enhancement is induced via the interaction of two optical frequencey tunable laser beams in the sample region. This method has only recently become feasible with the advent of the dye laser. In Section 3, we discuss more straightforward extensions of the Tobin method of Section 1. Tobin points out that the Raman signal to noise ratio will increase as the square root of the data acquisition time. However, we point out that the acquisition time is, in practice, restricted by various environmental factors. In Section 3, we discuss various practical methods of lengthening the acquisition time. One method, discussed in some detail, is signal chopping via electric field application. The effect of an electric field on Raman spectra is considerably stronger than its effect on fluorescence. The Electro-Raman Effect (ERE), experimentally, is a straightforward extension of the Tobin method. It has the advantage that additional complimentary data wiil be obtained.

## 1. Fluorescence Discrirnination via Counting

When Raman data are acquired superimposed on a fluorescence background, the intrinsic noise of the system results from the quantum nature of the incident photon flux. It is reasonably well known that the pulses from a photomultiplier caused by photons empinging on the cathode obey Poisson statistics. This has the following implication: suppose there is a fluorescence band superimposed on a Raman line, then the total average number of pulses, $N_T$, received by the photomultiplier will be approximately the average number of pulses due to the fluorescence, $N_F$, plus the

average number of pulses due to the Raman line $N_R$ ; thus $N_T \cong N_F + N_R$. The approximation results because there will be a mean statistical fluctuation of $(N_F + N_R)^{1/2}$ about $N_T$. Therefore, the intrinsic signal to noise ratio is given by the following equation.

$$\text{SNR} = \frac{N_R}{(N_F + N_R)^{1/2}} \tag{1}$$

The actual signal to noise ration will be somewhat less than this. One reason is that there can be other forms of noise that will cause the value of $N_T$ to fluctuate. Two examples of this are shot noise in the photomultiplier and intensity variation in the exciting source. Actually, shot noise via PM dark current can be made negligible by cooling the photomultiplier and laser fluctuations can be compensated as is discussed in Section 3. In addition to fluctuation noise on $N_T$, noise can be introduced in the electronic system following the photomultiplier tube. M. Tobin has pointed out that a pulse counting system will eliminate any noise not coming from fluctuations in $N_T$. Equation 1 is, therefore, seen to be the important equation describing signal to noise for a Raman line superimposed on a fluorescence background.

In the traditional spontaneous Raman effect, as discussed by Tobin, when data are acquired for biochemical samples, the fluorescence count is usually orders of magnitude larger than the Raman count. In this event, Eq. 1 reduces to:

$$\text{SNR} = \frac{N_R}{N_F^{1/2}} \tag{2}$$

Since the Raman and fluorescence counts are both linearly dependent on laser intensity, I, and counting time, t, Eq. 2 can be written:

$$\text{SNR} = \frac{o\, I t}{o, I t} = \frac{\sigma_R}{\sigma_F^{1/2}} I^{1/2} t^{1/2} \tag{3}$$

In this equation, $o$, and $\sigma_F$ are sample dependent quantities. Now, let us examine this equation for methods of increasing the SNR. There are three methods. The first is quite trivial. We observe that a higher laser power will increase the SNR. This, however, reaches a point of diminishing returns. The thermal lens effect, boiling, and destruction of the sample negate any gains achieved by increasing the laser power ad infinitum. The second method of increasing the SNR of Eq. 3 is by increasing the counting time, t. However, there is also an upper limit on $t$. This upper limit comes from environmental noise. The problems with environmental noise, i.e., sample vibrations, lens vibrations, spectrometer vibrations, temperature change,

etc., are not rasily resolved. Our experience indicates that counting times above 10 seconds are not profitable with respect to improving the SNR. However, $t$ can be considerably lengthened when chopping techniques are employed. This is discussed further in Section 3. The third method of increasing the SNR of Eq. 3 is to vary the sample dependent quantities, o, and o, from their thermal equilibrium values.

Tobin derives Eq. 3 and points out that with a pulse counting system this equation desci-ibes reasonably well experimental data he obtains from teflon and lysozyme. His experimental method is a traditional laser Raman method with pulse counting. For teflon, Tobin reports an N, of 2380 and an $N_R$ of 553 for an 8 sec counting time, $t$. He measures a standard deviation for 15 counting periods of 31 in reasonably good agreement with $N_T^{1/2} = 43$. Thus for $N_R/N_T = 0.3$, he finds a SNR of 15.

In the next section, the SNR of Eq. 3 is radically increased by selective phonon population. In effect, o, is increased and $\sigma_{\dot{F}}$ is made to approach zero.

## 2. Fluorescence Discrimination via Selective Phonon Population Enhancement

### a) The Method of Population Enhancement

Calculations given here, based on experimentally measured stimulated Raman cross sections[5] and the nitrogen laser pumped dye laser system described by Hansch[6], show that optical phonon populations can be selectively enhanced to the point that anti-Stokes Raman radiation can be easily detected. The selective phonon population enhancement is induced by two dye laser beams focused into the sample medium. The proposed experimental arrangement is shown in Figure 1. In the experimental geometry of Figure 1, the photon frequency, $\omega_s$ of dye laser 2 is set lower than the photon frequency of dye laser 1, $\omega_L$, by an amount equal to a phonon frequency for the sample material, $o_r$. In this case, in analogy with the stimulated Raman effect experiments described by N. Bloembergen[7], the beam from dye laser 1 can be considered to be the primary laser pump beam at $\omega_L$ and the beam from dye laser 2 can be considered to be the Stokes shifted beam at $\omega_s$. These two beams are coupled via the sample medium optical phonons at $\omega_p$. The result is that Iight from beam 1 is converted to beam 2 with a creation of optical phonons. If the phonon creation rate is larger than the phonon decay rate, the optical phonon

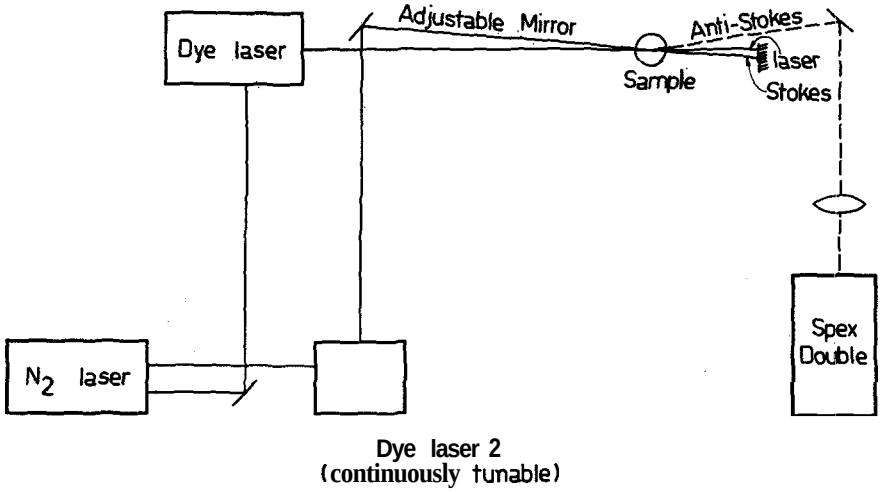


Fig. 1 - The experimental arrangement for the *selective* phonon population enhancement Raman technique is shown. Two $N_2$ laser pumped dye lasers provide the laser and Stokes beam for a stimulated Raman process. The process generates detectable anti-Stokes radiation.

population at $O$, will build up. Since the Raman cross section for light scattered on the anti-Stokes side is proportional to the phonon population, anti-Stokes radiation will be detected on the higher frequency side of the primary laser beam. Since the enhanced phonon population is selective, the sample temperature is not significantly raised. Thus the fluorescence interference on the anti-Stokes side of the primary laser beam will be negligible. A complete Raman Spectra of a sample can be recorded by simultaneously scanning the recording spectrometer and the frequency of dye laser 2 at 'equal rates in opposite directions.

The main question to be answered concerning this proposed technique is the following: since the method is nonlinear in the laser power densities, then how large are the required laser power densities? Although the power densities required for stimulated Raman experiments are quite large, the calculations in the main part of this section show that the power densities required for the above described spectroscopic technique are considerably smaller. There are two reasons for this. First, in a stimulated Raman experiment, the Stokes beam is not usually supplied. However, the conversion rate is proportional to a product invoíving the laser pump and Stokes beam power densities. Second, in stimulated Raman experiments, the interest has been in Raman lasers. In the proposed technique, the criterion

is detectibility rather than device utility. The tolerable signal levels are then much lower.

### b) Theoretical Description of the Enhancement Mechanism

As is well known, the Raman effect originates via a phonon modulation of the material polarizability, $\alpha_0$. Thus:

$$\alpha = \alpha_0 + \frac{\partial \alpha}{\partial A_p} A_p + \cdots, \tag{4}$$

where $A_p$ is a phonon vibrational coordinate. The polarization at the Stokes frequency is given as follows:

$$P_s = \frac{\partial \alpha}{\partial A_p} A_p E_L \tag{5}$$

Here, $E_L$ is the electric field of the optical pump. The free energy associated with the Stokes frequency is simply:

$$F = \frac{1}{2} E_s P_s = \frac{1}{2} \frac{\partial \alpha}{\partial A_p} A_p E_s E_L . \tag{6}$$

This term represents a coupling between the three harmonic oscillators represented by the Stokes field amplitude, $E_s$, the laser field amplitude, $E_L$, and the phonon field amplitude, $A_p$. From the Hamiltonian representing these oscillators including the above coupling term, one can derive the following rather intuitive equation:

$$\frac{\partial E_s}{\partial z} = \gamma_{Lp} E_L A_p^* . \tag{7}$$

In this equation, $z$ is the laser beam propagation direction and $\gamma_{Lp}$ is a proportionality constant. The solution of Eq. 7 gives the well known result that the number of Stokes scattered photons is proportional to the pump intensity and the phonon population term, $(n_p + 1)$. Here:

$$\begin{aligned} |E_L|^2 &\sim I_L && \text{Laser Pump Intensity,} \\ A_p^+ A_p &\sim (n_p + 1) && \text{Stokes Scattering (Phonon Creation),} \\ A_p A_p^+ &\sim n_p && \text{Anti-Stokes Scattering (Phonon Annihilation).} \end{aligned} \tag{8}$$

Also from the Hamiltonian, one can derive the following not so well known equation:

$$\frac{\partial A_p}{\partial z} = \gamma_{Ls} E_L E_s^* - \frac{A_p}{\tau_p}, \tag{9}$$

where $\tau_p$ is the phonon relaxation time. The first term on the right hand side of this equation is analogous to the right hand side of Eq. 7. Except for coupling of the optical phonon to a thermal reservoir, the Hamiltonian is symmetric in the three oscillator amplitudes $E_L$, E, and A,. Then the first term results by permuting A, and E, in Eq. 7. The second term on the right hand side of Eq. 9 is a phonon damping term resulting from coupling to the thermal reservoir. The first term in Eq. 9 is the driving term for the stimulated Raman effect. This is dominated by thermal effects for the case of the spontaneous Raman effect.

For the considerations of the present section, in the steady state, the left hand side of Eq. 9 is zero. Eq. 9 can then readily be solved for A, and the result substituted in Eq. 7. Thus:

$$\frac{\partial E_s}{\partial z} = \gamma_{Lp}\,\gamma_{Ls}\,\tau_p\,|E_L|^2\,E_s\,. \tag{10}$$

From this equation, it is apparent that there is a gain in the Stokes beam which is linearly dependent on the pump beam intensity. Thus:

$$I_s(z) = I_s(0)\ e^{gz},$$

where

$$\mathbf{9} = \beta\,|E_L|^2 \quad \text{and} \quad \beta = 2\,\gamma_{Lp}\,\gamma_{Ls}\,\tau_p\,. \tag{11}$$

The above derivation of Eq. 11 follows that of N. Bloembergen[7]. It has been presented here as a revue for clarity. The quantity, g, has been measured for several gases, liquids, and solids.

For the experiment of Figure 1, it is now necessary to relate g to the anti--Stokes field amplitude, E,. To accomplish this, it is noted that there is an analogue equation to Equation 7 for the anti-Stokes field amplitude, E, . Thus:

$$\frac{\partial E_a}{\partial z} = \gamma_{Lp}\,E_L^*\,A_p\,. \tag{12}$$

The solution of Eq. 9 for A, can be substituted in this equation as was done in Eq. 7. Then

$$\frac{\partial E_a}{dz} = \gamma_{Lp}\,\gamma_{Ls}\,\tau_p\,E_L^2\,E_s^* = \frac{1}{2}\,\beta\,E_L^2\,E_s^*\,. \tag{13}$$

Actually, there is a restriction implicit in Eq. 13. Momentum conservation is assumed. To write this explicity, it can be recalled that E, is an amplitude for a wave traveling as exp i $\mathbf{k}_a$ . r. Similar exponentials are applicable for E, and $E_L$ . Thus Eq. 13 is rewritten as follows[8]:

$$e^{i\mathbf{k}_a \cdot \mathbf{r}} \frac{\partial E_a}{\partial z} = \frac{\beta}{2} [E_L e^{i\mathbf{k}_L \cdot \mathbf{r}}]^2 \cdot E_s^* e^{-i\mathbf{k}_s \cdot \mathbf{r}} ; \quad (14)$$

therefore

$$e^{i\mathbf{k}_a \cdot \mathbf{r}} e^{i\mathbf{k}_s \cdot \mathbf{r}} \frac{\partial E_a}{\partial z} = \frac{1}{2} \beta E_L^2 E_s e^{2i\mathbf{k}_L \cdot \mathbf{r}}.$$

Then the momentum conservation condition is:

$$\mathbf{k}_s + \mathbf{k}_a = 2\mathbf{k}_L . \quad (15)$$

Figure 2 shows the momentum matching condition of Eq. 15. Via the sample medium dispersion, there is a small angle, $0,$, between $\mathbf{k}_L$ and k,. This angle will vary with the Stokes beam frequency, $w,$.

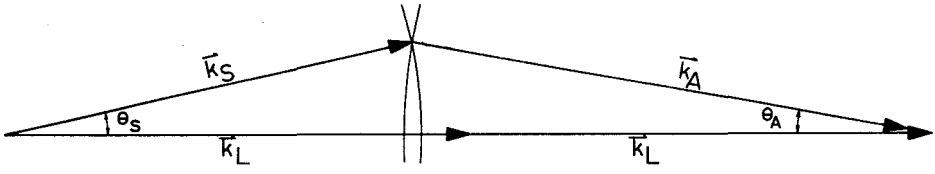


**Fig.** 2 - The angle. $\theta_s$, between the input laser and Stokes beams must be set such that thc anti-Stokes radiation generated can satisfy the momentum conservation condition shown here.

The requirement of momentum conservation is an important constraint in the experiment of Figure 1. The angle between the two input beams must be controlled. Actually, a slight variation in the angle $\theta_s$ between the laser and Stokes beams can be tolerated. This variation results because the length of **k,** varies slightly via the frequency variation in $\omega_a$ possibly as a result of the phonon decay width.

In the next subsection, calculations are made for the anti-Stokes count rate for a specific sample medium.

### c) Stimulated Anti-Stokes Count Rate for Benzene

As can be seen from Eq. 13, the anti-Stokes intensity is proportional to the Stokes power density and the square of the laser power density (See Eq. 17). It is profitable, then, to focus the Stokes and laser beams in order to increase the anti-Stokes intensity. However, there is a limit to this. The smaller the spot size, the larger the diffraction limited beam angles. The sum of the beam spreads can not exceed the angular variation allowable

in $\theta_s$ as discussed in the previous section. For a spot size too small, laser power will be wasted. To calculate the anti-Stokes count rate, it is necessary to begin with a calculation of the allowable variation in $\theta_s$.

The quantity, $\theta_s$, has been measured for calcite[g] (2.49") and for nitrobenzene 10 (3.1°), both with ruby laser light excitation. A value for benzene of about 2.5" seems to be appropriate. The 992 $cm^{-1}$ benzene half width is known to be 3.1 $cm^{-1}$ (Ref. 11). Thus $\Delta\mathbf{k}_a$ is 3.1 $cm^{-1}$. From the dot product of $\mathbf{k}_a$ with Eq. 15 and assuming $\theta_s = \theta_a$ in Figure 2, one finds:

$$\Delta\theta_s = \frac{\Delta k_a}{(2\mathbf{k}_i - \mathrm{k},) \sin\theta_s}. \tag{16}$$

For $k_L = 15000\,cm^{-1}$, then $\Delta\theta_s = 4 \times 10^{-3}$ rad. From this value of AO, and the standard formula relating diffraction angle and spot size[12], one finds a minimum spot radius of 50$\mu$.

Hansch[6] reports the construction of an extremely narrow line width dye laser. Using a Fabry-Pérot etalon inside the laser cavity, he finds a line width of .004 Å. However, he reports as well a line width narrowing to .30 Å using only an internal cavity telescope. For the aplication here, the internal cavity telescope laser is more than sufficient. For his dye laser. he reports 20% power conversion from a 100 kW peak pulse $N_2$ laser. The beam is near diffraction limited (2.5 m rad for a 80$\mu$ waíst size).

Eskin[5] et *al.* have measured g for benzene. They find a g value for the 932 $cm^{-1}$ line of .04 $cm^{-1}$ with an input laser power of 12 $MW/cm^2$.

For practical experimental reasons to be discussed later, we assume the two Hansch type dye lasers of Figure 1 to be focused down via cylindrical lens systems to interaction beams of width 300$\mu$ and height 3 mm. See Figure 3.

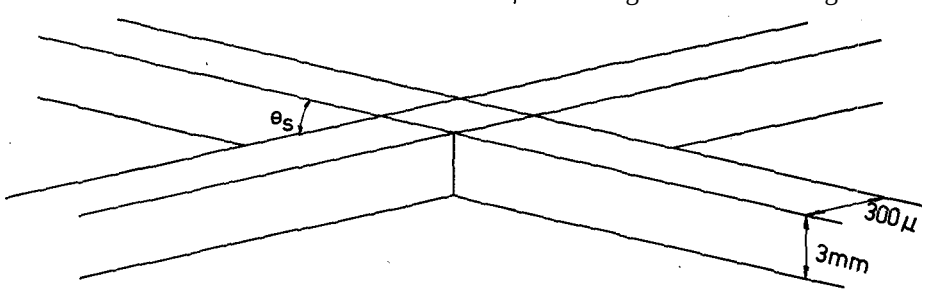


Fig. 3 - The intersection region of the laser and Stokes beams is shown. Since intersection of the two beams in the sample region is critical, the 3 mm beam height is chosen to facilitate allignment in that dimension.

Since the nitrogen laser beam in Figure 1 is split 50-50 each dye laser is capable of 10 KW peak power. For the geometry of Figure 3, one calculates a laser power density of 1 MW/cm$^2$. Equation 10 can be solved to yield the following value for the anti-Stokes intensity:

$$I_a = \frac{1}{4}\beta^2 |E_L|^4 I_s z^2 = \frac{1}{4} g^2 z^2 I_s . \tag{17}$$

Here, $z$ is the interaction length. For the present case, from $z = 300\,\mu/\sin\theta_s$, then $z = 3\,mm$. From the above values, $I_a$ is calculated for benzene.

$$I_a = \left[\frac{1}{2} \times \left(\frac{.04}{12}\right) \times 3 \times 10^{-1}\right]^2 I_s = 2.5 \times 10^{-7} I_s$$

This value can be converted to a count rate by noting that the average power from an Avco $N_2$ laser is 100 mW. Assuming a spectrometer efficiency of 1%, then the anti-Stokes count rate is: $i_a = 10^9$ cps.

Actually, since the anti-Stokes photons will be bunched up during the time duration of the laser pulses, the counts will not be resolvable. However, a DC electrometer system can be used. A pulse counting system can easily detect 2 or 3 cps and a DC system is only 2 or 3 times less sensitive. Thus, a signal to noise ratio for benzene of $10^8$ is predicted. This value is several orders of magnitude better than the SNR for benzene of a few times $10^4$, found in a spontaneous Raman experiment.

### d) Experimental Considerations

In this subsection, a possible experimental system is discussed. The experimental diagram of Figure 1 can be imagined split into two parts, the laser section and the sample section. Figure 4 shows the laser section, and Figure 5 shows the sample section.

The grating in dye laser 2 in Figure 4 is adjustable. It can be stepped with a stepping motor synchronized with the drive motor in the spectrometer of Figure 5. The lens system of Figure 4 processes the dye laser beam such that the focus is in the sample with beam dimensions as given in Figure 2. The cylindrical lens geometry for Figure 3 guarantees that the beams coincide in the sample. And since $\theta$ will vary as the Stokes and anti-Stokes frequencies vary it is necessary to adjust the position of mirror 1 in Figure 5 for each value of the spectrometer setting.

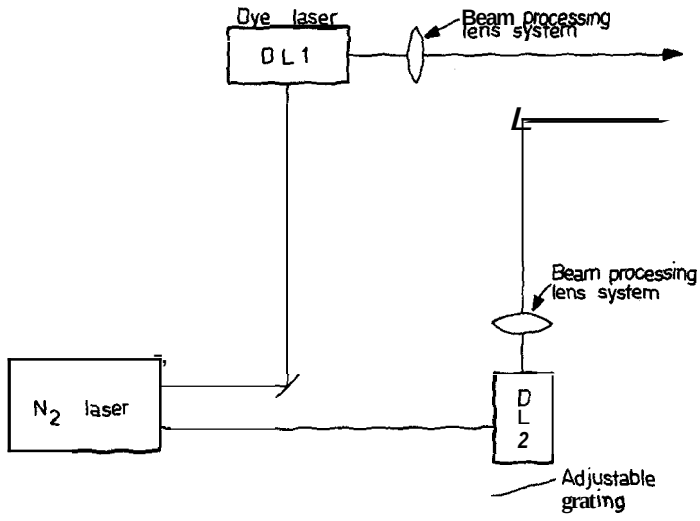


Fig. 4 - The experimental geometry of Figure 1 can be divided into two parts, the beam processing section and the sample spectroscopy section. The beam processing section is shown here. After processing two beams are provided with focused dimensions as shown in Figure 3.

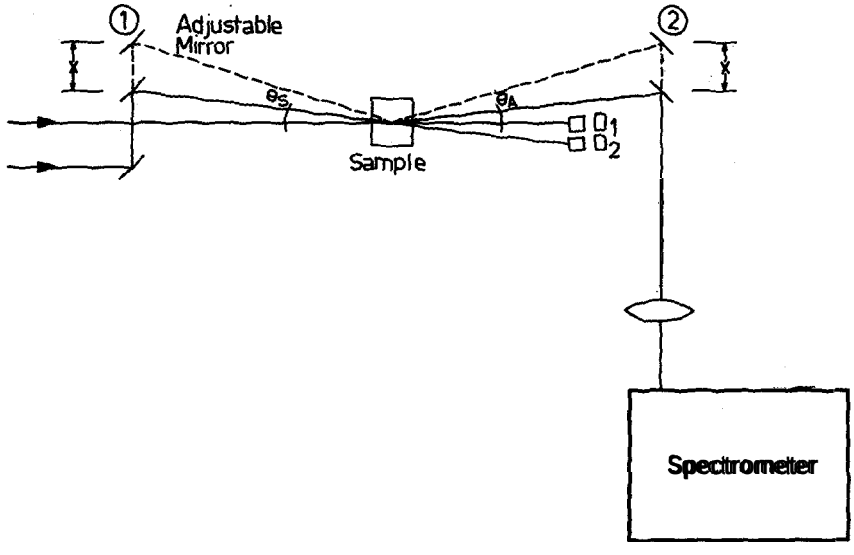


Fig. 5 - The sample spectroscopy section of Figure 1 is shown here. As the frequency of the Stokes beam is tuned, it is necessary to tune the positions and angles of mirrors 1 and 2 in accordance with the momentum matching condition of Figure 2. Detectors D, and $D_2$ allow the possibility of correction of laser pulse intensity fluctuations.

In order to focus the Stokes beam in the same sample region as $\theta$ is varied, it is necessary to change the mirror angle as the mirror position is changed. This can be accomplished, because in the small angle aproximation the angle variable is linearly related to the translation variable. Then, the required coupling can be done by means of a mechanical linkage. Mirror 2 is mounted in a similar fashion to mirror 1.

In Figure 5, when 2 is servoed to mirror 1 and if we assume $\theta_s = \theta_a$, then the spectrometer focusing lens will maintain the image of the sample region anti-Stokes light on the slit independent of 8. Actually, $\theta_s$ and $\theta_a$ are approximately equal[13]. For nitrobenzene, 0, $= 3°$ and $\theta_s - \theta_a = .1°$. Therefore, spectrometer slit widths of 100 $\mu$ should be sufficient. However, it should be noted that narrow spectrometér slit widths are not necessary. The resolution is determined by the angle definition in the sample. The spectrometer only serves as a means of filtering off laser and Stokes light.

The experimental procedure, then, is to step the spectrometer frequency simultaneously with the frequency of dye laser 2. For each frequency setting, the mirror position, x, is adjusted for maximum signal with a feedback Ioop to the spectrometer photomultiplier.

The material dependent quantity, $\beta$, can be measured by electronically processing the Stokes and laser beam power densities per pulse measured by detectors $D_1$ and $D_2$ with the anti-Stokes current signal per pulse.

### 3. Fluorescence Discrimination via Extended Counting Intervals

The experimental technique outlined in Section 2 is radically different from that conventionally used in spontaneous Raman effect experiments. Exploratory experiments are required to verify the utility of the technique. As of the present writing, high intensity Stokes and anti-Stokes radiation has been observed via stimulated effects when a high power laser beam, is incident on a sample, However, few two beam experiments have been reported. Biraud-Laval et *al.*[14] have reported a two beam dye laser experiment on quartz. They measure a Stokes gain but they make no attempt to observe anti-Stokes radiation. For the purpose of completeness, in in this Section, we study some more straightforward extensions of the method described by Tobin for the acquisition of Raman spectra for macromolecules.

**a) Laser Power Stabilization**

As we have discussed in Section 1, a data acquisition time in Eq. 3 longer than 10 sec does not usually increase the SNR. A major practical reason for this is the lack of good laser power stability. One method of increasing the power stability employed in some existing laser systems is to use a monitor of the laser power in a feed back loop from the power supply to the laser head. An alternative method is shown in Figure 6b.

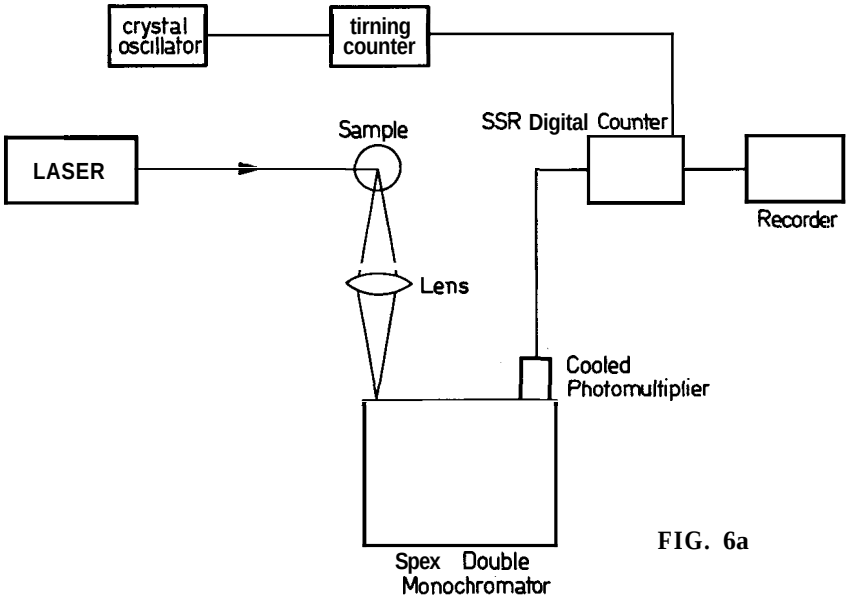


FIG. 6a

Fig. 6 - The pulse counting Raman experimental set up is shown. In 6a, the Tobin type system is presented where a crystal oscillator determines the counting interval. In 6b, the crystal oscillator is replaced by a laser photon detector. With the system of 6b, laser power fluctuations are automatically compensated. If a Solid State Radiation (SSR) digital synchronous computer is used, the crystal oscillator should be replaced by an externa1 time consisting of a laser photon monitor.

In Figure 6b, instead of a crystal oscillator timing device as in the Tobin system, shown in Figure 6a, a small percentage of the laser beam is collected by a beam sampler and fed to the timing counter. The digital counter continues to count until the timing device counts a present number of photons from the laser beam. The variation in laser intensity is compensated for by normalizing the count time. If the timing counter is set to count $10^8$ photons, an effectivelaser stability of 1 part in $10^4$ will be obtained.

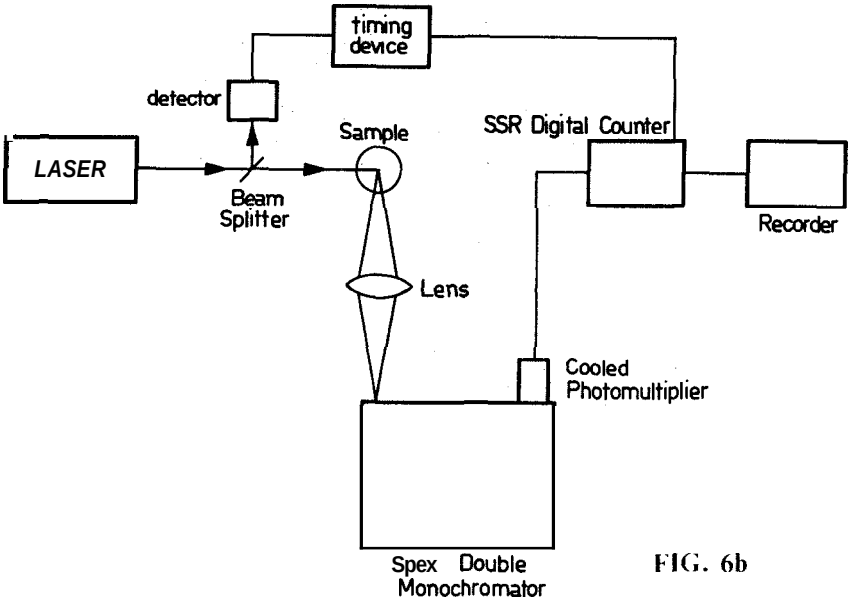


FIG. 6b

This stability is difficult to attain with a laser power supply feed back loop.

**b) The Tobin Chopping – Repeated Data Accumulation**

Tobin demonstrates that the limit of detection of Raman lines in a fluorescence background can be made arbitrarily small by effectively chopping the signal in the following manner. In the case of teflon and lysozyme fifteen observations were made with $t = 8$ seconds. First a reading was made on the Raman line, then on the background nearby; this technique essentially chops the signal and enables the experimenter to extend the effective $t$ as long as needed to retrieve the signal at the desired SNR.

Although Tobin apparently records the data by hand for selected Raman lines, there is no reason why this chopping system can not be automated by means of a stepping motor in the spectrometer drive system and a bidirectional counter in the detection system.
A programmed pulse generator can be used to step the spectrometer back and forth from one point to a neighboring point repeatedly until sufficient

data is accumulated; then the system can be advanced to a new point and the process repeated.

### c) The Electro-Raman Effect and Chopping

By a simple extension of the Tobin experimental set up of Fig. 6a, the SNR of Section 1 can be enhanced by means of a lengthening of integration time.

A high intensity square wave modulated electric field is applied to the sample. (The experimental set up is shown in Fig. 7). Although in comparison with the method of Section 3b, this electric field method of accumulating Raman data gives a lower SNR for equal acquisition times, the electro Raman effect has the advantage that it provides further characterization information.

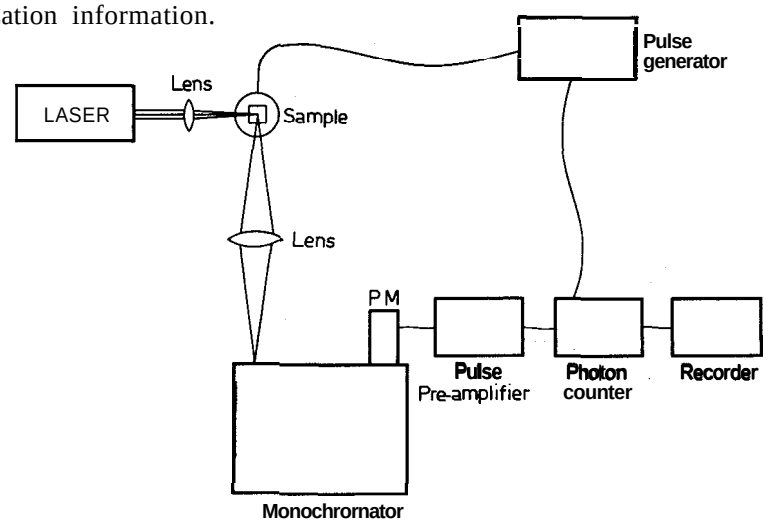


Fig. 7 - The experimental set up for the electro-Raman effect is shown. The set up is essentially the same as that of 6a with the addition of a electric field source. (A Cober model 605-P is recommended). If a SSR digital synchronous computer is employed as the counting system, the necessary provision for chopping is provided.

The application of an electric field modifies the symmetry of the optical phonons and thereby modifies polarization selection rules for the first order Raman scattèring. This is manifested in the spectra as induced Raman effects plus enhancement or degradation of existing Raman lines.

We now set out to discuss some of the experimental and theoretical aspects of measuring the electric field Raman effect, ERE, on larger molecules

assuming a fluorescence background. It is recognized that it would be advantageous to apply the externa1 field E, at some frequency f > 100 Hz in order to remove the measured signal from the environmental noise mentioned previously. We are therefore faced with retrieving a signal above the background which is the difference between the Raman signal with and without the applied electric field. The signal to noise for such an experiment can be estimated as follows:

$$\text{SNR} < \frac{\Delta N_T}{(N_F + N_R)^{1/2}} = \frac{N_R(E_A) - N_R(E_A = 0) + N_F(E_A) - N_F(E_A = 0)}{(N_F + N_R)^{1/2}}$$

$$= \frac{[\eta_R(E_A) - \eta_R(E_A = 0) + \eta_F(E_A) - \eta_F(E_A = 0)]\, t^{1/2}}{(\eta_F + \eta_R)^{1/2}} \qquad (18)$$

where the quantity $\eta$ is the count rate.

The count rate is now expanded in terms of the field:

$$\eta(E_A) = \eta(E_A = 0) + \sum_{n=1}^{\infty} \frac{1}{n!} \left( \frac{\partial^n \eta}{\partial E_A^n} \right) E_A^n \qquad (19)$$

Now substituting Equation 19 into Equation 18, one gets

$$\text{SNR} < \frac{\left[ \sum_{n=1}^{\infty} \frac{1}{n!} \left( \frac{\partial^n \eta_R}{\partial E_A^n} \right) E_A^n + \sum_{n=1}^{\infty} \frac{1}{n!} \left( \frac{\partial^n \eta_F}{\partial E_A^n} \right) E_A^n \right] t^{1/2}}{(\eta_F + \eta_R)^{1/2}}. \qquad (20)$$

The electrochromic effect will be quadratic in the field[15,16] which Peduces the expansion of $\eta_F(E_A)$ as follows

$$\eta_F(E_A) = \frac{1}{2} \left( \frac{\partial^2 \eta_F}{\partial A_A^2} \right) E_A^2 . \qquad (21)$$

The electro-Raman effect can be either linear or quadratic in the field[17,18] depending on the system under study.

The expansion of $\eta_R(E_A)$ becomes

$$\eta_R(E_A) = \left( \frac{\partial \eta_R}{\partial E_A} \right) E_A + \frac{1}{2} \left( \frac{\partial^2 \eta_R}{\partial E_A^2} \right) E_A^2 \qquad (22)$$

and it can be seen that there will be two SNRs, depending on the effect. One SNR occurs at the frequency, *f*, of the applied field. This is the linear effect. The SNR at 2f results from the quadratic effect:

$$\mathrm{SNR}_f < \left(\frac{\partial \eta_R}{\partial E_A}\right) E_A\, t^{1/2} \tag{23}$$

$$\mathrm{SNR}_{2f} < \frac{\frac{1}{2}\left[\left(\frac{\partial^2 \eta_R}{\partial E_A^2}\right) E_A^2 + \left(\frac{\partial^2 \eta_F}{\partial E_A^2}\right) E_A^2\right] t^{1/2}}{(\eta_F +} \tag{24}$$

We will just concern ourselves with the estimation of $\mathrm{SNR}_{,,}$. Frist, it is realized that the intensities of the fluorescence background and the Raman line are directly proportional to their respective count rates, r], and r], , i.e.,

$$I_{F\cdot} = a\,\eta_F\,, \qquad I_R = a\,\eta_R\,.$$

We begin the numerical estimate of $\mathrm{SNR}_{2f}$ by citing literature information concerning $\Delta I_F/I_F$ :

$$(\Delta I_F/I_F) = \frac{I_F(E_A) - I_F(E_A = 0)}{\langle I_F \rangle} = \frac{\eta_F(E_A) - \eta_F(E_A = 0)}{\langle \eta_F \rangle}$$

$$\cong \left(\frac{\partial^2 \eta_F}{\partial E_A^2}\right) \frac{E_A^2}{2\eta_F} \cong 10^{-4}.$$

Here, $10^{-4}$ is taken as a lower limit of the detectivity magnitude for the electrochromic effect for fields in the neighborhood of $10^5$ v/cm (Refs. 16, 19-23). The effect of the electric field on fluorescence is thus seen to be quite weak. For the expression $\left(\frac{\partial^2 \eta_R}{\partial E_A^2}\right)\frac{E_A^2}{2\eta_R}$ and fields of $10^5$ v/cm, the literature reports cases of 20% enhancement of the Raman line[17]. So in most cases the fluorescence term in the numerator for the $\mathrm{SNR}_{2f}$ expression can be dropped. However, as will be seen in Fig. 8, this is not an important condition.

Now we will calculate the SNR at $2f$ using the Tobin data for teflon given in Section 1. Thus, for $\eta_R = 30\%$ r], , Eq. 24 can be written as follows:

$$\mathrm{SNR}_{2f} < \frac{\frac{1}{2}\left[\frac{\partial^2 \eta_R}{\partial E_A^2} E_A^2\right] t^{1/2}}{4\eta_R^{1/2}} \simeq \frac{1}{2}\,\eta_R^{1/2}\,(0.2)\,t^{1/2}.$$

For the Tobin teflon data, r], = 70 counts/sec. With a time constant of $t = 100$ sec, $\mathrm{SNR}_{2f}$ is 9.

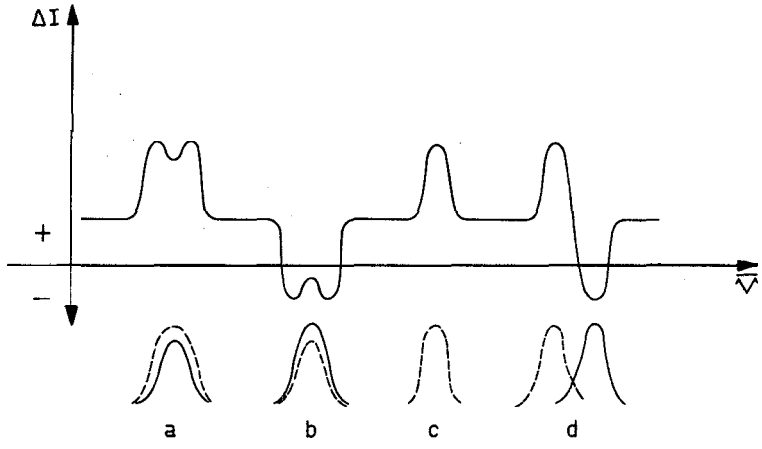


Fig. 8 - A sample electro-Raman effect spectra is shown in the upper section of this figure. In the lower section, the solid line represents a Raman line with zero field. The dotted line represents the Raman line in the presence of a high field. In *a*, the field increases the Raman intensity and in b, it decreases the intensity. In c, Raman activity is induced by the field, and in *d*, the field induces a phonon frequency shift.

This drop in the SNR[24] from Section 1 can be compensated by the acquisition of additional information. See figure 8. The effects of the applied field will manifest themselves as changes in the scattering strength of a particular Raman mode; see areas a and b of Fig. 8. However, there will also be changes in Raman selection rules and splitting of degeneracies of the optical phonons. These are shown in areas c and *d* respectively of Fig. 8. In Fig. 8 it has been assumed that **AI,** is not negligible and is manifested as a positive signal, although it could be negative. Since the fluorescence bands are very broad, the signal **AI,** is slowly varying with frequency. Figure 8 also shows how the shape of the ERE signal implies the nature of the electric field perturbation on the Raman mode.

In Figure 7, the experimental set up is given that would give the best ERE results in SNR. The digital system is recommended since it has essentially drift free operations in the electronics following the photomultiplier and the standard pulse shaper. This allows for very long integration time. of the order of hours, if needed. In our system (Figure 7) it was seen that $t$ needed to be of the order of 50-100 seconds. The duration of the gate is equal to or smaller than the pulse width of the electric field, $E_A$, and in a chopping system only short term stability is required.

## Conclusions

The disadvantages of the two proposed experimental techniques are (1) in the case of the phonon enhancement, a system must be constructed to comply with the experimental requirements and (2) for the electro-Raman effect, investments in money for a good electric field supply ($ 5.000) and in time for learning techniques of applying high fields to samples are required. A third (3) problem lies in the area of interpretation of acquired data.

Although with simple organic molecules, a well known application of Raman data is in the use of vibrational analysis as a tool to accomplish structure elucidation, it may be impossible to assign spectra of macromolecules, due to their complexity, to fundamental modes. It will be possible in many cases with good spectra to identify functional groups. Also, "finger print spectra" without interpretation will be valuable in medical diagnostics.

The enhanced phonon population technique is most promising. In the following, some of the potential advantages of the proposed enhanced phonon Raman effect are discussed for the case of biochemical samples.

### 1. Feasability of Dilute Samples

Biochemical samples are probably most often in the form of dilute samples in water solution. The classical Raman scattering intensity is proportional to the molecular concentration. This statement is still valid for the phonon enhanced Raman process discussed above. Then a benzene dilution of 1 part in $10^8$ is theoretically tolerable. Even though benzene is a stronger Raman scatterer than most organic molecules, dilute samples can certainly be run.

### 2. Spectrum Sharpening

The quantity $\beta$ is proportional to the Raman cross section, $\sigma$, and the phonon life time, $\tau_p$. Since the sharp features in a Raman spectrum are the features with large phonon lifetimes, the enhanced phonon Raman effect will enhance the sharp features. Thus, perhaps with this method, sharp features can be extracted from the broad bands in large organic molecules.

## 3. Experimental Simplicity

For dilute samples, the momentum matching condition of Figure 2 is dependent on the index of refraction of the solvent. Then the angle $\theta_s$ is nearly independent of the solute and different biochemical samples can be run in succession with small changes in the experimental setup. This may allow computer solutions of the value of x as a function of frequency instead of a feedback loop for x.

## 4. Resonant Raman Enhancement

The fact that the primary laser beam frequency in Figure 1 originates from a dye laser opens up the possibility of tuning the primary laser frequency through the visible spectrum. There is experimental Raman work indicating that when the laser exciting frequency is tuned to the frequency of a chromophoric absorption band, the chromophoric phonon modes are greatly enhanced. For example, in nitrobenzene, the NO, phonon is strongly enhanced as the laser frequency shifts to the blue[13]. In the classical Raman effect, fluorescence becomes a problem as one approaches absorption bards. As mentioned earlier, fluorescence will not be a problem on the anti-Stokes side of the laser frequency.

It has been shown in this paper that with modified experimental techniques, the acquisition of Raman data of macromolecules is quite possible.

The authors havc profited from valuable discussions with Dr. P. Frazer Williams, Dr. Jose Salzberg and Dr. Herndon Williams.

### References and Notes

1. I. R. Beatie, Chem. in Britain **3,** 347 (1967).
2. K. W. F. Kohlrausch, ***Ramanspektren,*** Acad. Verlag Becker and Erler, Leipzig (1943).
3. P. S. Hendra, H. **A.** Willis and H. Zichi, ***Polymer,*** in Press.
***4.*** M. C. Tobin, J. Op. Soc. Am., 58, 1057 (1968).
5. V. A. Eskin, M. L. Kats, N. K Sidorov, and Yu. P. Turbin, Opt. Spectrosc., **26,** 571 (1969).
6. T. W. Hansch, Applied Optic., **11,** 895 (1972).
7. N. Bloembergen, ***Nonlinear*** *Optics*, W. A. Benjamin Inc.. N. Y. (1965).
8. The exponential on the LHS of Eq. 14 appears outside of the derivative because the Maxwell equation involved is second order and reduced to first order with the assumption that the variation of E over wave length is small. See Ref. 7, p. 86.
9. R. Chiao and B. Stoicheff, Phys. Rev. Letters, **12,** 290 (1964).
10. See Ref. 7, P. 157.
11. See Ref. 7, p. 151.

**12.** A. Yanv, Quantum Electronics, J. Wiley and Sons, Inc., N. Y. **225 (1967).**
**13.** P. P. Sorokin and W. V. Srnith, ***The*** Laser, McGraw-Hill Book Co., N. Y., Section **4-4 (1966).**
**14. S. Biraud-Laval, *G.*** Chartier, and R Reinisch, *Light* Scattering in Solids, Edited by M. Balkanski, Flammarion Sciences p. **197 (1971).**
**15.** J. **R.** Platt, J. Chem Phys., 34, **862** (1960).
**16.** H. Labhart, Chimie (Switzerland), 15, **20 (1961).**
17. E. Anastassakis, A. Filler, and E. Burstein, Light Scattering of Solids, Edited by Wright, **421 (1969).**
**18. E. U.** Condon, Phys., Rev. **41, 759 (1932).**
**19.** The value $10^{-4}$ has been reported for the electrochromic effect on many different systems. Two examples are:

a) TCNE-benzene charge transfer complex, J. E. Moore and D. A. Dows, to be published.
b) Methyl red, J. Kumamoto, J. C. Powers, Jr., and W. R Heller, J. Chem. Phys., **36,2893 (1962).**

**20.** G. Chiarotti. U M. Grassano, and R. Rosei, Phys. Rev Letters, 20. **1043 (1966).**
**21. J. R.** Platt, J. Chem Phys., **34, 3 (1961).**
**22.** W. Liytay and J. Czekalla, Z. Elektrochem., **65, 121 (761).**
**23. J.** C. Powers, J. Kurnamoto, and W. R. Heller, J. Arn. Chem Soc., **86,** 1004 **(1964).**
**24.** In fact, the $SNR_{2f}$ value of **9 can** be enhanced further by lengthening t. (For t = **10** min, the $SNR_{2f}$ becomes **22).**